

## Deliquescence Behavior of Multicomponent Aerosols

Zhaozhu Ge,<sup>†</sup> Anthony S. Wexler,<sup>\*,†</sup> and Murray V. Johnston<sup>‡</sup>

Department of Mechanical Engineering and Department of Chemistry and Biochemistry, University of Delaware, Newark, Delaware 19716

Received: July 23, 1997; In Final Form: October 27, 1997<sup>⊗</sup>

The deliquescence behavior of multicomponent aerosols has been studied extensively by measuring the particle size or weight growth at controlled relative humidities. To our knowledge there has been no experimental investigation of the chemical composition of the aerosol surface as a function of relative humidity, which is extremely important in understanding a number of issues in atmospheric chemistry and physics. Rapid single-particle mass spectrometry (RSMS) has been used in this work to explore the deliquescence behavior of particles generated from NaCl/KCl, NaCl/NaNO<sub>3</sub>, and (NH<sub>4</sub>)<sub>2</sub>SO<sub>4</sub>/NH<sub>4</sub>NO<sub>3</sub> mixed solutions and then conditioned at different relative humidities. Thermodynamic predictions of the crystallization/deliquescence behavior of each mixture were also given. For NaCl/KCl and NaCl/NaNO<sub>3</sub> mixtures, the data were generally consistent with thermodynamic analysis and earlier investigations. The results indicate that as the ambient relative humidity reaches the deliquescence point of the system, the chemical composition of the particle surface changes gradually with increasing relative humidity until the particle transforms completely to an aqueous droplet. The observed deliquescence began at relative humidities somewhat lower than that predicted by equilibrium thermodynamics. This is probably due to the cracks on the particle surface. The deliquescence behavior of (NH<sub>4</sub>)<sub>2</sub>SO<sub>4</sub>/NH<sub>4</sub>NO<sub>3</sub> mixtures observed was very complicated and was generally not consistent with thermodynamic predictions.

### Introduction

A knowledge of the deliquescence behavior of multicomponent aerosols is important in understanding and modeling the atmospheric processes affecting air quality, visibility, and climate change. Inorganic salts comprise 25–50% of atmospheric fine aerosol mass, and most of the inorganic salts exhibit deliquescence behavior upon exposure to a humid environment.<sup>1</sup> In recent years substantial research has been reported on the phase transformation and growth of aerosol particles composed of mixed salts as a function of ambient relative humidity and temperature.<sup>2–11</sup>

For aerosol particles containing a single salt, the phase transformation from solid to aqueous solution occurs at a specific relative humidity, generally referred to as the deliquescence relative humidity (DRH).<sup>7</sup> The deliquescence behavior of multicomponent aerosol particles is much more complicated. To explore the deliquescence behavior, we have to understand the opposite phase transition—efflorescence. Ge et al.<sup>12</sup> described the mechanism of multicomponent aerosol crystallization and the chemical composition and morphology of the resulting dry particles in detail. Briefly, let us consider two salts in solution. As the ambient relative humidity is lowered, one of the salts eventually becomes saturated, and its crystalline phase forms. As the relative humidity is further lowered, more of the solid phase of this salt forms, and the residual solution becomes more concentrated in the other salt. At a certain relative humidity, referred to as the mutual deliquescence relative humidity (MDRH),<sup>7</sup> the two salts crystallize together and form a mixed solid phase at the eutonic composition.<sup>12</sup> The

MDRH is always lower than the DRH of individual solutes.<sup>7</sup> The resulting dried particles are composed of a pure salt core surrounded by a mixed salt coating, where the core composition is solely determined by the original aerosol composition, but the coating is identical with the eutonic composition and is independent of the original aerosol composition.

If the ambient relative humidity is increased, the size of the dried particle remains unchanged until the relative humidity reaches the MDRH, at which point the partial pressure of water in the atmosphere becomes identical with the water activity of the eutonic.<sup>2</sup> The solid coating having eutonic composition at the particle surface is then dissolved in the absorbed water. Due to surface tension, the remaining pure salt solid core stays at the center of the particle and is surrounded by saturated solution of eutonic composition. Further increasing the relative humidity results in more water absorption into the particle, and part of the pure salt solid core is dissolved to maintain water equilibrium between the solution and the atmosphere. At a certain relative humidity, which is a function of the overall composition of the original particle, the pure salt solid core is completely dissolved into the solution, and the particle becomes a pure aqueous droplet.

As we have shown, the surface solution composition of a multicomponent aerosol particle undergoing deliquescence keeps changing until a certain relative humidity is reached. Therefore, the deliquescence behavior of multicomponent aerosols affects a number of atmospheric processes such as fog formation, cloud physics, equilibrium vapor pressure, and mass-transfer kinetics of trace gases. Previous experimental work studied the deliquescence behavior of multicomponent aerosol particles by continuously monitoring the changes in weight or the optical characteristics of a single suspended droplet undergoing controlled growth.<sup>1–4,5,6,8,9</sup> The chemical composition of the

<sup>†</sup> Department of Mechanical Engineering.

<sup>‡</sup> Department of Chemistry and Biochemistry.

<sup>⊗</sup> Abstract published in *Advance ACS Abstracts*, December 1, 1997.

resulting aqueous solution on the particle surface during deliquescence is still experimentally unknown although thermodynamic models are available.<sup>7,13</sup> Recently, a new technique (rapid single-particle mass spectrometry, RSMS) has been reported by Johnston and Wexler<sup>14</sup> for on-line analysis of single aerosol particles based upon laser desorption/ionization. The aerosol is sampled through a differentially pumped inlet into a time-of-flight mass spectrometer. Each particle is detected in the source region by light scattering of a continuous helium–cadmium laser beam and then ablated in-flight by an excimer laser. The resulting ions are accelerated into the mass spectrometer, and a mass spectrum is recorded. Due to the short delay (less than 1 ms) between sampling and analysis, chemical transformation and contamination of particles during sampling are minimized.

Carson et al.<sup>15,16</sup> indicated that RSMS can be used to analyze the particle surface composition and monitor chemical reactions. Ge et al.<sup>12</sup> used this technique to explore the surface chemical composition and morphology of particles dried from multicomponent solutions. Neubauer et al.<sup>17,18</sup> studied aqueous aerosols by ablating the particles with 248 and 193 nm excimer laser radiation. Their results suggested that RSMS is capable of probing the deliquescence behavior of multicomponent aerosols. In this work we use RSMS to explore the deliquescence behavior of three groups of multicomponent aerosols containing NaCl/KCl, NaCl/NaNO<sub>3</sub>, and (NH<sub>4</sub>)<sub>2</sub>SO<sub>4</sub>/NH<sub>4</sub>NO<sub>3</sub>, which are common constituents of atmospheric aerosol particles.

### Experimental Section

The experimental methods, instrumentation, and setup employed in this investigation have been described in detail elsewhere.<sup>15,17,18</sup> Generally, monodisperse aerosols of a known size and composition were produced from a vibrating orifice aerosol generator (Model 3450; TSI, St. Paul, MN). A solution containing the desired amounts of respective salts plus 1:1 (v:v) mixture of ethanol and water solvent was fed into the generator. The generated droplets were subsequently exposed to a stream of dry air at relative humidity less than 3% for approximately 4 s which removed the solvent, yielding a monodisperse dried aerosol of solute particles. Particle size distribution was monitored with an aerodynamic particle sizer (Model 3310; TSI, St. Paul, MN). The mean dry particle diameters of all aerosols studied were around 3.5 μm and fairly monodispersed ( $\sigma < 0.3 \mu\text{m}$ ).

The dry particles then passed through a relative humidity controlled annular laminar flow reaction chamber which was connected to the differentially pumped mass spectrometer inlet. The humidity system was very similar to that described by Neubauer et al.<sup>17</sup> except for a few modifications. Saturated air was prepared by bubbling dry air through temperature controlled water, with subsequent cooling, and then mixed with the aerosol-carrying air flow. The relative humidity and temperature were continually monitored with an hygrometer (Model HT205W; Rotronic Instrument Corp., Huntington, NY) which was located near the mass spectrometer inlet. The desired relative humidity was obtained by adjusting the relative flow rates of saturated and dry particle-containing air. The adjustable range of relative humidity was 7%–94%. Note that although the relative humidity of the air used to dry the aerosol was below 3%, substantial water evaporated from the droplets during the drying process increased the final relative humidity in the reaction chamber to 7% even if no saturated air was added. The relative humidity measurements were accurate to within 1%, although some of the particles may have experienced higher relative

humidities for a short time during the flow mixing process. The particles stayed in the reaction chamber for approximately 1 min before entering the mass spectrometer. This time was sufficient for particles to reach equilibrium with the water vapor in the carrier air flow. The particles were then sampled into the mass spectrometer and exposed to vacuum for about 1 ms before undergoing laser desorption/ionization with an 193 nm excimer laser (Model PSX-100; MPB Technologies, Dorval, Quebec, Canada) for chemical characterization.

In this study, all chemicals were used without further purification: sodium chloride (Mallinckrodt), sodium nitrate (Aldrich), potassium chloride (Mallinckrodt), ammonium sulfate (Aldrich), and ammonium nitrate (Aldrich). Spectra for (NH<sub>4</sub>)<sub>2</sub>SO<sub>4</sub>/NH<sub>4</sub>NO<sub>3</sub> and NaCl/NaNO<sub>3</sub> were obtained in the negative ion mode; spectra for KCl/NaCl were obtained in the positive ion mode.

### Results and Discussion

**KCl/NaCl.** The solubility diagram of this system was constructed by Tang.<sup>2</sup> From the solubility curves, it was determined that the eutonic point for this system is at the mole fraction NaCl:KCl = 7:3. Tang et al.<sup>3</sup> experimentally found a value of 0.738 for the water activity at the eutonic point (MDRH) of the NaCl/KCl system. Cohen et al.<sup>5</sup> confirmed these values and extended the water activity data for this system to higher solution concentrations. Both of them observed that the dry particle of NaCl/KCl was anhydrous and contained only two pure crystalline phases of NaCl and KCl. Ge et al.<sup>12</sup> using RSMS studied the crystallization process of this system and observed the eutonic point. To elucidate the deliquescence behavior of this system, let us define  $X_{\text{KCl}} = m_{\text{KCl}}/(m_{\text{KCl}} + m_{\text{NaCl}})$  as the relative solute mole fraction. The eutonic composition point is then at  $X_{\text{KCl}} = 30\%$ . Consider an aqueous droplet of composition  $X_{\text{KCl}} = 10\%$  subjected to decreasing relative humidity. For relative humidities lower than the MDRH, a dried particle forms that is composed of a pure NaCl core surrounded by a coating of eutonic composition with  $X_{\text{KCl}} = 30\%$ .<sup>12</sup> If this dried particle is subjected to an increase in relative humidity, the particle will remain unchanged until MDRH is reached. The coating having eutonic composition at the particle surface is then dissolved in the absorbed water. Due to surface tension, the remaining pure NaCl solid core stays at the center of the particle and is surrounded by saturated solution with  $X_{\text{KCl}} = 30\%$ . Further increasing the relative humidity results in more water absorbed into the particle, and part of the pure NaCl solid core is dissolved to maintain the water equilibrium between the solution and the atmosphere. The relative mole fraction ( $X_{\text{KCl}}$ ) of the solution decreases as the relative humidity increases. At a certain relative humidity, which is close to but lower than the DRH of pure NaCl (75.7%), the NaCl solid core is completely dissolved into the solution, and the particle becomes an aqueous droplet with  $X_{\text{KCl}} = 10\%$ .

For aqueous particles originally having  $X_{\text{KCl}} > 30\%$ , say 50%, the crystallization and deliquescence behavior are similar to  $X_{\text{KCl}} = 10\%$ , but the core of the dried particle is pure KCl. Thus, the relative mole fraction ( $X_{\text{KCl}}$ ) of the solution increases as the relative humidity increases. At a certain relative humidity, which is between MDRH of this system (73.8%) and DRH of pure KCl (84.3%), the pure KCl solid core is completely dissolved into the solution, and the particle becomes an aqueous droplet with  $X_{\text{KCl}} = 50\%$ .

If  $X_{\text{KCl}}$  happens to be 30%, the eutonic composition of this system, the particle crystallizes or deliquesces like pure salt at relative humidity of 73.8%. The phase transformation either

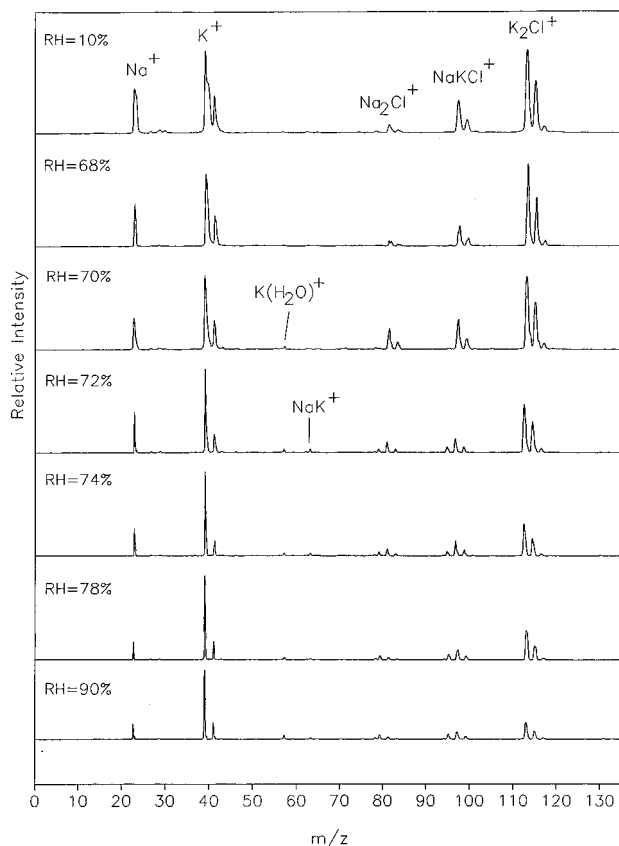


**Figure 1.** Averaged positive ion spectra of 40 particles dried from an aqueous droplet of NaCl/KCl mixture with  $X_{\text{KCl}} = 50\%$  and then conditioned at various relative humidities. The laser fluence was  $0.4 \text{ J/cm}^2$ . Mean particle diameter was  $3.5 \mu\text{m}$ .

from aqueous to solid or from solid to aqueous occurs abruptly. The dried particles of this composition are morphologically and chemically uniform.<sup>12</sup>

In this study, we generated particles containing NaCl and KCl, with the relative KCl mole fractions of 10%, 30%, and 50%, and applied  $0.4 \text{ J/cm}^2$  laser fluence to each sample. The relative humidities ranged from 10% to greater than 90%. At least 40 successive single particles were analyzed with the same nominal operating conditions (generated from same solution, prepared with same relative humidity, and ablated at same laser fluence). Figure 1 displays the positive ion spectra of particles generated from a solution of NaCl and KCl in a 1:1 mole ratio ( $X_{\text{KCl}} = 50\%$ ) and then conditioned at various humidities. Each spectrum is the average of 40 individual spectra obtained at the identical operating conditions. Averaging was performed to observe all the trends.<sup>18</sup> At a relative humidity of 10%, the particles stay dry and the spectrum is very similar to what we have detected with 248 nm laser fluence;<sup>12</sup> both simple cations ( $\text{Na}^+$ ,  $\text{K}^+$ ) and cluster ions ( $\text{Na}_2\text{Cl}^+$ ,  $\text{NaKCl}^+$ ,  $\text{K}_2\text{Cl}^+$ ) are observed. As the relative humidity increased to 68%, the spectrum is essentially the same as at a humidity of 10% except for noticeable decreases of ion intensity to all the peaks probably due to adsorbed water. At a relative humidity of 70%, a new peak due to  $\text{K}(\text{H}_2\text{O})^+$  ( $m/z$  57) appears and confirms that water has been adsorbed on the particle surface. At relative humidity of 72%, the spectrum changes dramatically, with substantial decreases of ion intensity in all peaks. This phenomenon suggests that significant amounts of water reside on the particle surface, which changes the laser desorption/ionization mechanism and ion yields.<sup>17,18</sup> Particulate water also induces peak narrowing in the mass spectra which can be attributed to

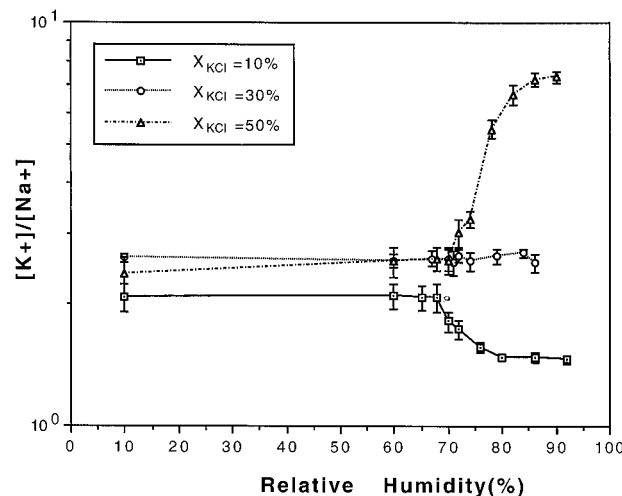


**Figure 2.** Peak area ratio of  $[\text{K}^+]/[\text{Na}^+]$  versus relative humidity for particles generated from solutions with  $X_{\text{KCl}} = 10\%$ , 30%, and 50%. The laser fluence was  $0.4 \text{ J/cm}^2$ . Mean particle diameter was  $3.5 \mu\text{m}$ . Each data point is the average of at least 40 spectra. The error bars indicate the standard error of the mean.

translational cooling from the increased water content in the plume.<sup>17,19</sup> Further relative humidity increases lead to decreasing intensity of the peak due to  $\text{Na}^+$  ( $m/z$  23) and other peaks due to cluster ions. Note that the ion intensity of the peak due to  $\text{K}^+$  ( $m/z$  39,  $m/z$  41) remains nearly constant for those spectra. Therefore, the peak area ratio of  $[\text{K}^+]/[\text{Na}^+]$  increases as the relative humidity increases. This observation indicates that the relative mole fraction of KCl on the particle surface increases as relative humidity increases.

Even at relative humidities far above the MDRH, where the particle contains a substantial aqueous phase, water clusters (e.g.,  $\text{H}(\text{H}_2\text{O})_n^+$ ) are not observed. The only peak associated with water  $\text{K}(\text{H}_2\text{O})^+$  ( $m/z$  57) remains weak even at high relative humidity. During the laser desorption/ionization process, ions such as  $\text{Na}^+$  and  $\text{K}^+$  are readily formed in the plume because the corresponding neutrals have low ionization potentials. Water clusters are not observed because the initial step in their formation, ionization of vapor-phase  $\text{H}_2\text{O}$ , is inhibited by its high ionization potential. Furthermore, the high-energy environment of the plume favors cluster dissociation (i.e., evaporation) rather than condensation.

To further explore the changes of particle surface composition during deliquescence, the peak area ratios of  $\text{K}^+$  ( $m/z$  39) and  $\text{Na}^+$  ( $m/z$  23) were calculated for each spectrum to indicate the relative mole ratio of components. Figure 2 shows the peak area ratio ( $[\text{K}^+]/[\text{Na}^+]$ ) versus relative humidity. Each data point represents the average of at least 40 spectra of identical particles. For particles generated from solutions with  $X_{\text{KCl}} = 10\%$ , the peak area ratio of  $[\text{K}^+]/[\text{Na}^+]$  remains constant until relative humidity reaches 70%. Then the peak area ratio decreases gradually, and at relative humidities beyond 76% the peak area ratio remains constant with increasing relative humidity, indicating that the particle has completed the phase transition to an aqueous droplet, in agreement with the thermodynamic analysis.

For particles generated from solutions with  $X_{\text{KCl}} = 30\%$ , i.e., eutonic composition, the peak area ratio generally does not change as a function of relative humidity. The data suggest that particles of this specific composition are chemically uniform. For particles generated from solutions with  $X_{\text{KCl}} = 50\%$ , the peak area ratio of  $[\text{K}^+]/[\text{Na}^+]$  remains constant until the relative humidity reaches 70%. Then the peak area ratio increases gradually, and at relative humidities beyond 86% the

peak area ratio generally no longer changes, showing that the particle was completely dissolved.

Standard error of the mean for each data point also has been shown in Figure 2. The particle-to-particle fluctuations probably result from pulse-to-pulse inhomogeneities within the excimer laser beam, phase distribution, and morphology. Mansoori et al.<sup>20</sup> showed that averaging a greater number of particles could lower the error.

Generally, we have observed that NaCl/KCl system shows apparent deliquescence behavior, and the experimental results are consistent with thermodynamic predictions. Our data also indicated that a significant quantity of water was in the particles at a relative humidity of 68%–70%, significantly lower than the deliquescence relative humidity of 74% observed by Tang et al.<sup>3</sup> using an optical particle counter and Cohen et al.<sup>5</sup> using electrodynamic balance. The differences imply that substantial water has been adsorbed on the particle surface at relative humidities lower than the MDRH since RSMS is known to be surface sensitive.<sup>15,16</sup> Similar phenomena were reported by other researchers on the surface of pure NaCl aerosols. Vogt and Finlayson-Pitts<sup>21</sup> using diffuse reflectance infrared Fourier transform spectrometry observed that significant amounts of water reside on the pure NaCl aerosol surface at a relative humidity of 53.8%, far below the deliquescence relative humidity of pure NaCl salt (75.7%). Neubauer et al.<sup>18</sup> found water on pure NaCl aerosol at a relative humidity of 70% using the same apparatus as this study. Other work also confirms these observations.<sup>22,23</sup>

Water on the surface of aerosol particles at relative humidities lower than the deliquescence point may change the reaction kinetics of aerosols with trace gases.<sup>21</sup> Barraclough and Hall<sup>22</sup> studied the adsorption of water vapor by NaCl at room temperature and found that a monolayer of water was adsorbed on the salt surface at relative humidities lower than the deliquescence point. They proposed two-dimensional condensation and a concept of “active sites” on the surface as a most reasonable interpretation of their experimentally derived water vapor adsorption isotherms. It is unlikely that the water on the surface of aerosol particles at a relative humidity lower than the deliquescence point observed in the present study was due to the same mechanism of water vapor adsorption on NaCl surface proposed by Barraclough and Hall.<sup>22</sup> RSMS probably would not be able to detect this small amount of water based on previous studies in our group.<sup>16,18</sup>

The condensational growth of aerosol particles during the expansion of carrier gas in the mass spectrometer inlet may introduce water on the particle surface. Neubauer et al.<sup>18</sup> using the condensational growth model developed by Mallina et al.<sup>24</sup> determined that, at the relative humidity of 70%, only a 2 nm thick layer of water condenses on the particle surface. This amount of water would not be detectable by RSMS. Also, the water layer on the particle surface introduced by condensation grows linearly with the increases of relative humidity of carrier gas. Therefore, the spectrum should change smoothly which contradicts our observations.

A reasonable interpretation of our observations may be that the aerosol particles generated by the vibrating orifice aerosol generator (Model 3450; TSI, St. Paul, MN) contain substantial cracks and even pores on the particle surface.<sup>25,26</sup> The cracks on the surface may increase the adsorption of water significantly due to surface tension lowering of water activity in pores. Pruppacher and Klett<sup>27</sup> pointed out that aerosol particles contain air capillaries in which condensation of water vapor proceeds at a relative humidity lower than the deliquescence relative

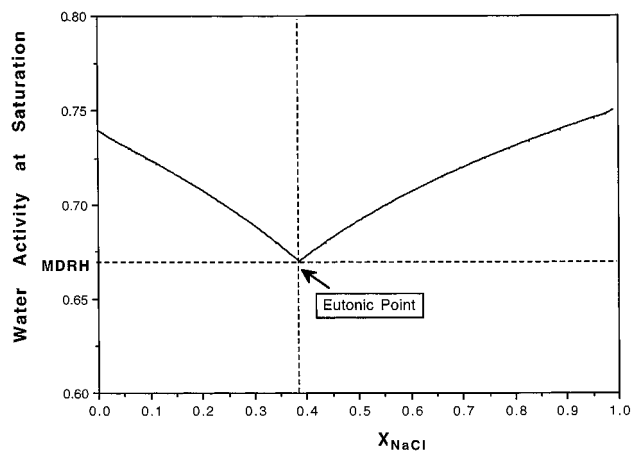


**Figure 3.** Water activity at saturation of an aqueous solution of NaCl and NaNO<sub>3</sub> at 25 °C.

humidity. Considering that the meniscus of water in a capillary is concave, in contrast to the convex surface of a water drop, and applying the Kelvin equation, we have

$$RH = a_w \exp\left(-\frac{2M_w\sigma_{w/a}}{RT\rho_w r}\right)$$

where RH is the relative humidity,  $a_w$  is the water activity in the capillary,  $M_w$  is the water molecular weight,  $\sigma_{w/a}$  is the surface tension,  $R$  is the universal gas constant,  $T$  is the absolute temperature,  $\rho_w$  is the density of water, and  $r$  is the radius of curvature of water surface in the capillary. The equation shows that the water activity inside the cracks is always lower than the deliquescence relative humidity due to the negative curvature, and also the smaller the crack size, the lower the equilibrium pressure of water over it. Therefore, at a certain relative humidity lower than the deliquescence relative humidity, sufficient water has been adsorbed into the cracks on the particle surface to be detectable by RSMS. For the NaCl/KCl system, this transition happened at around 68%–70% relative humidity. It can be estimated by using the equation that the crack size to reduce the water vapor pressure over the crack to the observed value is about 30 nm, which is reasonable considering the 3.5  $\mu\text{m}$  particle diameter.

**NaCl/NaNO<sub>3</sub>.** Atmospheric NaCl comes from the evaporation of sea spray produced by bursting bubbles or wind-induced wave breaking action.<sup>28</sup> The reactions of NaCl aerosols with NO<sub>2</sub>, HNO<sub>3</sub>, and N<sub>2</sub>O<sub>5</sub> in the atmosphere produce NaNO<sub>3</sub> solids.<sup>21</sup> Using Aerosol Inorganics Model II (AIM II, URL: <http://www.me.udel.edu/wexler/aim.html>),<sup>7,13</sup> we can plot the water activity at saturation of the NaCl/NaNO<sub>3</sub> system versus  $X_{\text{NaCl}} = m_{\text{NaCl}}/(m_{\text{NaCl}} + m_{\text{NaNO}_3})$  at 25 °C (see Figure 3). The eutonic point for this system is  $X_{\text{NaCl}} = 37.8\%$ , with a corresponding MDRH of 67%. The thermodynamic analysis of the deliquescence behavior of this system is very similar to that of the NaCl/KCl system.

The deliquescence behavior of the particles that we studied was consistent with theoretical analysis. Three mixtures of NaCl/NaNO<sub>3</sub> with relative NaCl mole fraction at 20%, 37.8%, and 80% have been investigated. A laser fluence of 0.4 J/cm<sup>2</sup> was applied to each sample. The relative humidities ranged from 10% to 76% and higher. At least 40 successive single particles were analyzed with the same nominal operating conditions. Figure 4 displays the negative ion spectra of particles generated from a solution with a relative NaCl mole fraction of 80% and then conditioned at various relative

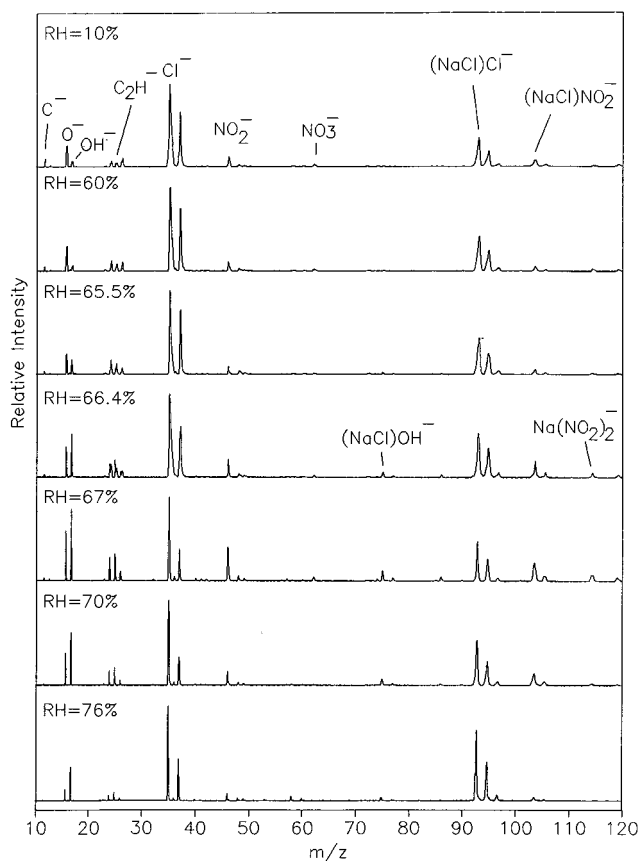


**Figure 4.** Averaged negative ion spectra of 40 particles dried from an aqueous droplet of NaCl/NaNO<sub>3</sub> mixture with  $X_{\text{NaCl}} = 80\%$  and then conditioned at various relative humidities. The laser fluence was 0.4 J/cm<sup>2</sup>. Mean particle diameter was 3.5  $\mu\text{m}$ .

humidities. At a relative humidity of 10%, the particles remained dry, and peaks corresponding to C<sup>-</sup>, O<sup>-</sup>, OH<sup>-</sup>, C<sub>2</sub>H<sup>-</sup>, Cl<sup>-</sup>, NO<sub>2</sub><sup>-</sup>, NO<sub>3</sub><sup>-</sup>, NaCl<sub>2</sub><sup>-</sup>, and (NaCl)NO<sub>2</sub><sup>-</sup> were observed. The C<sup>-</sup>, OH<sup>-</sup>, and C<sub>2</sub>H<sup>-</sup> peaks may be attributed to the ethanol solvent or organic contamination during aerosol preparation.<sup>18,29</sup> Note that the intensity of the OH<sup>-</sup> peak is much lower than that of O<sup>-</sup>. As the relative humidity increases to 60%, the spectrum is essentially identical with the spectrum at a humidity of 10%. At a relative humidity of 65.5%, the intensity of the OH<sup>-</sup> peak increases, and a new but very weak peak due to (NaCl)OH<sup>-</sup> ( $m/z$  75) appears, indicating that water has been adsorbed on the particle surface. At 66.4% relative humidity, the spectrum changes significantly. The OH<sup>-</sup> peak becomes larger than the O<sup>-</sup> peak, the (NaCl)OH<sup>-</sup> peak appears, and the peak due to cluster ion (NaCl)NO<sub>2</sub><sup>-</sup> grows. All the changes imply that substantial water has been adsorbed on the particle surface. At a relative humidity of 67%, the spectrum changes dramatically, with substantial decreases of ion intensity to all the peaks. This observation suggests that significant amounts of water reside on the particle surface—the presence of an aqueous solution changes the laser desorption/ionization mechanism and yields.<sup>17,18</sup> Further relative humidity increases lead to decreasing NO<sub>2</sub><sup>-</sup> ion intensity ( $m/z$  46) while the Cl<sup>-</sup> ion intensity ( $m/z$  35,  $m/z$  37) remains nearly constant. Therefore, the peak ratio of [Cl<sup>-</sup>]/[NO<sub>2</sub><sup>-</sup>] increases with relative humidity, indicating that the relative mole fraction of NaCl on particle surface increases as relative humidity increases.

To further explore the changes of particle surface composition during the deliquescence process, peak areas of Cl<sup>-</sup> ( $m/z$  35,  $m/z$  37), NO<sub>2</sub><sup>-</sup> ( $m/z$  46), and NO<sub>3</sub><sup>-</sup> ( $m/z$  62) were measured, and the peak area ratio ( $m/z$  35 +  $m/z$  37):( $m/z$  46 +  $m/z$  62)

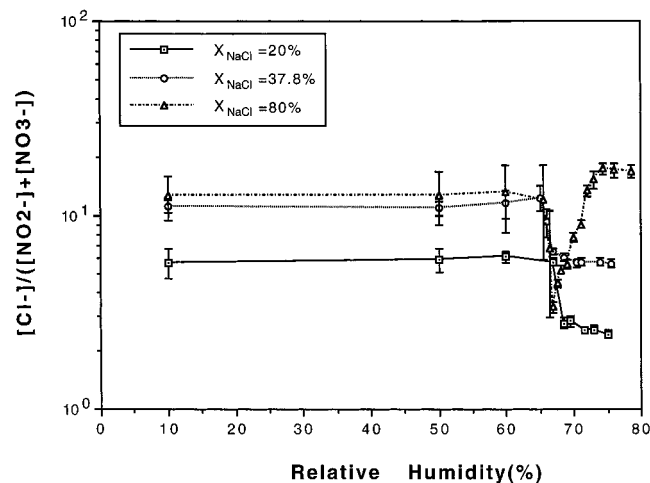


**Figure 5.** Peak area ratio of [Cl<sup>-</sup>]/([NO<sub>2</sub><sup>-</sup>] + [NO<sub>3</sub><sup>-</sup>]) versus relative humidity for particles generated from solutions with  $X_{\text{NaCl}} = 20\%$ , 37.8%, and 80%. The laser fluence was 0.4 J/cm<sup>2</sup>. Mean particle diameter was 3.5  $\mu\text{m}$ . Each data point is the average of at least 40 spectra. The error bars indicate the standard error of the mean.

was calculated for each spectrum to indicate the relative mole ratio of components. Figure 5 displays a plot of this ratio versus relative humidity. Each data point represents the average of at least 40 spectra of identical particles. For particles generated from solutions with  $X_{\text{NaCl}} = 20\%$ , the peak area ratio ([Cl<sup>-</sup>]/([NO<sub>2</sub><sup>-</sup>] + [NO<sub>3</sub><sup>-</sup>])) remains unchanged until the relative humidity reaches 66%. The peak area drops significantly as the relative humidity increases to 67%. Then the ratio decreases gradually with increasing relative humidity, implying that the mole fraction of NaNO<sub>3</sub> in the solution increases as the relative humidity increases.

For particles generated from solutions of eutonic composition where  $X_{\text{NaCl}} = 37.8\%$ , the peak area ratio remains generally constant in the range of measurement error until the relative humidity reaches 66%. The ratio then drops suddenly. But after the relative humidity reaches 67%, as we continue to increase the relative humidity, the peak area ratio basically remains unchanged. The data suggest that the particles changed from dry state to aqueous solution abruptly. The larger peak area ratio in the dry state may be attributed to the higher ionization sensitivity of sodium chloride than of sodium nitrate in the mixed crystal, as we also observed from spectra that the Cl<sup>-</sup> peak was much stronger than the peaks due to NO<sub>2</sub><sup>-</sup> and NO<sub>3</sub><sup>-</sup>. For particles generated from solutions with  $X_{\text{KCl}} = 80\%$ , the peak area ratio ([Cl<sup>-</sup>]/([NO<sub>2</sub><sup>-</sup>] + [NO<sub>3</sub><sup>-</sup>])) remains constant until the relative humidity reaches 66%. The peak area ratio drops suddenly as the relative humidity increases to 67%, indicating that a solution forms on the particle surface. Then the data increase gradually as the relative humidity increases, suggesting that more NaCl is dissolved. At relative humidities beyond 75%, the peak area ratio does not change much with relative humidity, indicating that the particle is a pure aqueous droplet.

Similar to the NaCl/KCl system, we observed that the deliquescence of this system occurred at relative humidity around 66%, less than the predicted value of 67% which may not represent a significant difference considering the accuracy in the relative humidity system. The mole fraction of solution formed on the particle surface during deliquescence changes gradually over a range of relative humidities except when the original aerosol composition is at the eutonic point. Vogt and Finlayson-Pitts<sup>21</sup> studied the reactions of NaCl aerosols with NO<sub>2</sub>, HNO<sub>3</sub>, and N<sub>2</sub>O<sub>5</sub>. They found that a quasi-liquid layer

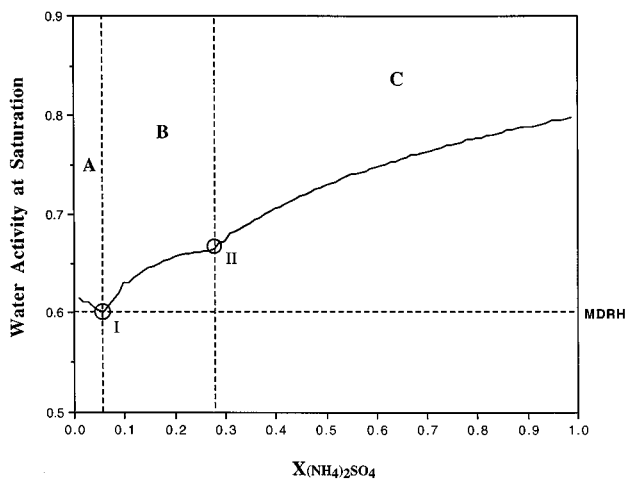


**Figure 6.** Water activity at saturation of an aqueous solution of  $(\text{NH}_4)_2\text{SO}_4$  and  $\text{NH}_4\text{NO}_3$  at 25 °C.

on the particle surface was formed even at water vapor pressure below the NaCl deliquescence point. They also discovered that, on drying of the particles, the reactions of NaCl with  $\text{NO}_2$  and  $\text{HNO}_3$  form  $\text{NaNO}_3$  crystals on the surface of the NaCl, thus regenerating fresh NaCl surface for future reactions. They concluded that this recrystallization may explain why sea salt particles totally depleted of chloride are often observed in the marine atmosphere. Considering the deliquescence behavior of the NaCl/ $\text{NaNO}_3$  system, it is clear that if the relative humidity decreases below the MDRH, crystallization results in a dry particle composed of a pure salt core and shell of eutonic composition ( $X_{\text{NaCl}} = 37.8\%$ ), where the core composition is solely determined by the composition of the particle. Thus, recrystallization generates a surface that always contains a fixed fraction of crystalline NaCl. As the relative humidity and temperature cycle repeatedly,  $\text{NO}_2$ ,  $\text{HNO}_3$ , and  $\text{N}_2\text{O}_5$  react with the NaCl on the particle surface, produce more  $\text{NaNO}_3$ , deplete more chloride from the particle, and release it into the atmosphere. It is possible that via this mechanism some sea salt particles are totally depleted of chloride.

**$(\text{NH}_4)_2\text{SO}_4/\text{NH}_4\text{NO}_3$ .** The deliquescence behavior of mixed  $(\text{NH}_4)_2\text{SO}_4/\text{NH}_4\text{NO}_3$  aerosols is much more complicated than for KCl/NaCl and NaCl/ $\text{NaNO}_3$  mixtures. Figure 6 shows the water activity at saturation of  $(\text{NH}_4)_2\text{SO}_4/\text{NH}_4\text{NO}_3$  system versus  $X_{(\text{NH}_4)_2\text{SO}_4} = m_{(\text{NH}_4)_2\text{SO}_4}/(m_{(\text{NH}_4)_2\text{SO}_4} + m_{\text{NH}_4\text{NO}_3})$  at 25 °C.<sup>12</sup> In region A ( $X_{(\text{NH}_4)_2\text{SO}_4} < 0.06$ ), the dried particle is composed of an  $\text{NH}_4\text{NO}_3$  solid core surrounded by an  $(\text{NH}_4)_2\text{SO}_4 \cdot 2\text{NH}_4\text{NO}_3/\text{NH}_4\text{NO}_3$  mixture. Thus, the relative mole fraction ( $X_{(\text{NH}_4)_2\text{SO}_4}$ ) of the solution decreases as the relative humidity increases during deliquescence. For droplets whose original mole fraction is in region B ( $0.06 < X_{(\text{NH}_4)_2\text{SO}_4} < 0.28$ ), the dried particles are composed of an  $(\text{NH}_4)_2\text{SO}_4 \cdot 2\text{NH}_4\text{NO}_3$  core surrounded by a mixture of  $(\text{NH}_4)_2\text{SO}_4 \cdot 2\text{NH}_4\text{NO}_3$  and  $\text{NH}_4\text{NO}_3$ . The relative mole fraction ( $X_{(\text{NH}_4)_2\text{SO}_4}$ ) of the solution increases as the relative humidity increases. If the original droplet mole fraction is in region C ( $X_{(\text{NH}_4)_2\text{SO}_4} > 0.28$ ), the dried particles are composed of an  $(\text{NH}_4)_2\text{SO}_4$  solid core surrounded by a layer of  $(\text{NH}_4)_2\text{SO}_4 \cdot 2\text{NH}_4\text{NO}_3$  and  $(\text{NH}_4)_2\text{SO}_4$ . Similar to compositions in region B, the relative mole fraction ( $X_{(\text{NH}_4)_2\text{SO}_4}$ ) of the solution increases as the relative humidity increases.

If  $X_{(\text{NH}_4)_2\text{SO}_4}$  happens to be at one of the two eutonic compositions (6% and 28%), the particle crystallizes or deliquesces like a pure salt at a relative humidity of 60% (eutonic point I) or 66% (eutonic point II). The phase transformation either from aqueous to solid or from solid to aqueous occurs

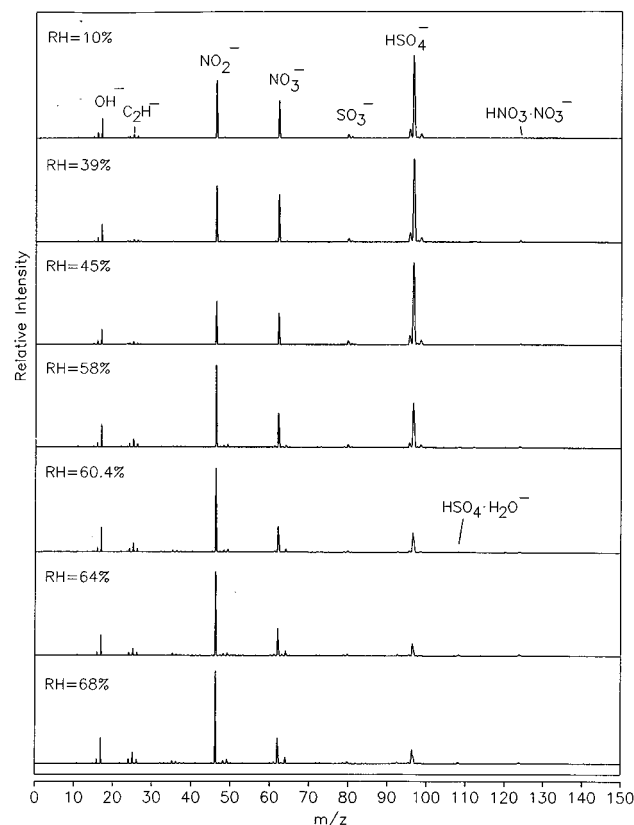


**Figure 7.** Averaged negative ion spectra of 30 particles dried from an aqueous droplet of  $(\text{NH}_4)_2\text{SO}_4/\text{NH}_4\text{NO}_3$  mixture with  $X_{(\text{NH}_4)_2\text{SO}_4} = 50\%$  and then conditioned at various relative humidities. The laser fluence was  $0.6 \text{ J/cm}^2$ . Mean particle diameter was  $3.5 \text{ }\mu\text{m}$ .

abruptly. The dried particles of this composition are morphologically and chemically uniform.<sup>12</sup>

Six mixtures of  $(\text{NH}_4)_2\text{SO}_4/\text{NH}_4\text{NO}_3$  with relative  $(\text{NH}_4)_2\text{SO}_4$  mole fraction at 2%, 6%, 20%, 28%, 50%, and 80% have been investigated. A laser fluence of  $0.6 \text{ J/cm}^2$  was applied to each sample. At least 30 successive single particles were analyzed with the same nominal operating conditions. Figure 7 shows the negative ion spectra of particles generated from a solution with relative  $(\text{NH}_4)_2\text{SO}_4$  mole fraction at 50% and then conditioned at various relative humidities. Each spectrum is the average of 30 individual spectra that were obtained at the identical operating conditions. At a relative humidity of 10%, peaks of  $\text{O}^-$ ,  $\text{OH}^-$ ,  $\text{C}_2\text{H}^-$ ,  $\text{NO}_2^-$ ,  $\text{NO}_3^-$ ,  $\text{SO}_3^-$ ,  $\text{HSO}_4^-$ , and  $\text{HNO}_3 \cdot \text{NO}_3^-$  are observed. The  $\text{C}_2\text{H}^-$  peak may be attributed to the ethanol solvent or organic contamination during aerosol preparation.<sup>18,29</sup> We do not observe the abrupt spectral intensity change at higher relative humidities as was observed in the NaCl/KCl and NaCl/ $\text{NaNO}_3$  systems. A very weak peak of  $\text{HSO}_4 \cdot \text{H}_2\text{O}^-$  appears in the spectra of particles at relative humidities higher than 60%.

To further investigate particle surface composition changes during the deliquescence process, the peak area ratio of  $[\text{HSO}_4^-] (m/z 97):([\text{NO}_2^-] (m/z 46) + [\text{NO}_3^-] (m/z 62))$  was determined for each spectrum to indicate the relative mole ratio of components. Figure 8 displays this peak area ratio versus relative humidity for particles at  $X_{(\text{NH}_4)_2\text{SO}_4} = 2\%$ , 6%, 20%, 28%, 50%, and 80%. The data show that factors other than thermodynamic equilibrium may contribute to the experimental results. In Figure 8a, where  $X_{(\text{NH}_4)_2\text{SO}_4} = 2\%$ , the peak area ratio decreases gradually as the relative humidity increases to 60% and then drops relatively faster until relative humidity reaches 64%. The peak area ratio does not change much at

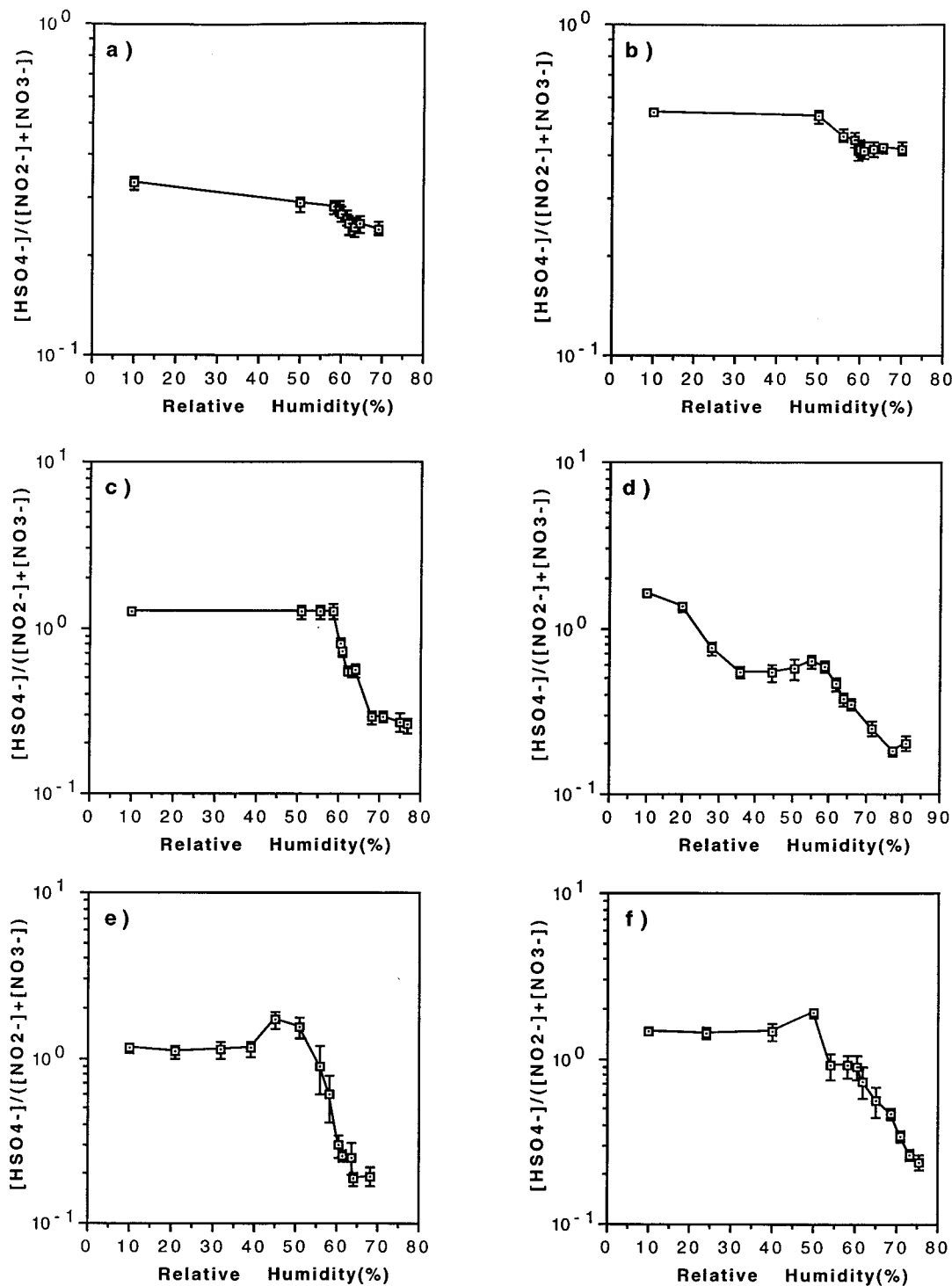


**Figure 8.** Peak area ratio of  $[\text{HSO}_4^-]/([\text{NO}_2^-] + [\text{NO}_3^-])$  versus relative humidity for particles generated from solutions with (a)  $X_{(\text{NH}_4)_2\text{SO}_4} = 2\%$ , (b)  $X_{(\text{NH}_4)_2\text{SO}_4} = 6\%$ , (c)  $X_{(\text{NH}_4)_2\text{SO}_4} = 20\%$ , (d)  $X_{(\text{NH}_4)_2\text{SO}_4} = 28\%$ , (e)  $X_{(\text{NH}_4)_2\text{SO}_4} = 50\%$ , and (f)  $X_{(\text{NH}_4)_2\text{SO}_4} = 80\%$ . The laser fluence was  $0.6 \text{ J/cm}^2$ . Mean particle diameter was  $3.5 \mu\text{m}$ . Each data point is the average of at least 30 spectra. The error bars indicate the standard error of the mean.

higher relative humidities. Although the trend of deliquescence is obvious, the thermodynamic analysis predicts that the peak area ratio should not decrease when the relative humidity is lower than the MDRH, which is 60% for this system. The difference between thermodynamic prediction and experimental data implies that some other factors contribute to the particle water absorption. Even at a relative humidity lower than the MDRH, the particle absorbs water and exhibits hygroscopic behavior. Similar observation has been reported by ten Brink and Veeffkind.<sup>30</sup>

The deliquescence behavior of  $\text{NH}_4\text{NO}_3$  is difficult to observe

experimentally. The data reported by Tang<sup>1</sup> indicated that pure  $\text{NH}_4\text{NO}_3$  aerosols are more hygroscopic than deliquescent. ten Brink and Veeffkind<sup>30</sup> observed the crystallization point of pure  $\text{NH}_4\text{NO}_3$  aerosol particles to be lower than 10%. The particles may exist as metastable aqueous droplets instead of thermodynamically favored dry particles even at the lowest relative humidity (around 10%) in this study.<sup>31</sup> Neubauer et al.<sup>18</sup> employed a similar apparatus as this study and confirmed that  $\text{NH}_4\text{NO}_3$  contains water, even at very low relative humidity. They observed that  $\text{NH}_4\text{NO}_3$  aerosols undergo a gradual phase transformation from dry to wet particles. ten Brink and

Veefkind<sup>30</sup> also investigated the deliquescence behavior of aerosols with 1:1 and 1:5 mixture of  $(\text{NH}_4)_2\text{SO}_4/\text{NH}_4\text{NO}_3$  and found that the 1:5 mixture did not show deliquescence or crystallization and thus behaved  $\text{NH}_4\text{NO}_3$ -like. Therefore, the particles with  $X_{(\text{NH}_4)_2\text{SO}_4} = 2\%$  and  $6\%$  (see Figure 8b) were more likely metastable aqueous droplets rather than dry particles even at the lowest relative humidities studied.

Figure 8c shows the peak area ratio of  $[\text{HSO}_4^-]/([\text{NO}_2^-] + [\text{NO}_3^-])$  versus relative humidity for particles with  $X_{(\text{NH}_4)_2\text{SO}_4} = 20\%$ , which is in the region B of Figure 6. The peak area ratio generally does not change until the relative humidity reaches 60%, where the ratio drops suddenly. As the relative humidity becomes higher than 68%, the curve flattens. The data show that significant phase change happened at relative humidity of 60%. But the peak area ratio drops during deliquescence rather than increases, contrary to what we expected from thermodynamic predictions. This may be due to known complications in the laser ablation process. Neubauer et al.<sup>17,18</sup> reported that the effect of water on laser desorption/ionization process may complicate the interpretation of experimental results.

As indicated by the data shown in Figure 8d for aerosols with  $X_{(\text{NH}_4)_2\text{SO}_4} = 28\%$ , the second eutonic composition, the particles behaved hygroscopically at relative humidities ranging from 10% to 35%. The particles generally remained unchanged as the relative humidity increased from 35% to 58%. Then the ratio drops gradually, indicating that more water has been absorbed into the particles.

For aerosols with  $X_{(\text{NH}_4)_2\text{SO}_4} = 50\%$ , which is in the region C of Figure 6, the peak area ratio data (see Figure 8e) are particularly interesting. The curve goes up at relative humidity of 40% and then drops gradually until the relative humidity reaches 60%. The curve flattens at higher relative humidities. The data indicate that the particle surface absorbed substantial amounts of water at relative humidities much lower than the corresponding relative humidity at the eutonic point II, which is around 66%. The data in Figure 8f ( $X_{(\text{NH}_4)_2\text{SO}_4} = 80\%$ ) show similar trends.

Thermodynamic equilibrium alone cannot explain the deliquescence behavior that we have observed for the mixtures of  $(\text{NH}_4)_2\text{SO}_4/\text{NH}_4\text{NO}_3$ . As we have proposed, the low crystallization point of  $\text{NH}_4\text{NO}_3$  may cause the particles at relative humidities lower than the MDRH to exist as metastable aqueous droplets. Thus, the  $(\text{NH}_4)_2\text{SO}_4/\text{NH}_4\text{NO}_3$  mixture aerosols may exhibit both hygroscopic and deliquescent behavior simultaneously. Other factors, such as the complexity of laser desorption/ionization mechanism, may contribute to uncertainties interpreting the experimental data.<sup>18, 32,33</sup>

## Conclusion

The deliquescence behavior of three multicomponent aerosols,  $\text{NaCl}/\text{KCl}$ ,  $\text{NaCl}/\text{NaNO}_3$ , and  $(\text{NH}_4)_2\text{SO}_4/\text{NH}_4\text{NO}_3$ , has been studied theoretically and experimentally. The results of the two relatively simple systems,  $\text{NaCl}/\text{KCl}$  and  $\text{NaCl}/\text{NaNO}_3$ , confirmed the thermodynamic analysis and were consistent with observations reported by other researchers. As the ambient relative humidity reaches the theoretical deliquescence point of that system, the chemical composition of the solution on the particle surface changes gradually with increasing relative humidity until the particle completes the transition to an aqueous droplet. The deliquescence observed for both systems began

at relative humidities somewhat lower than predicted by theory. Cracks formed on the surface of dry particles during their generation may contribute to this phenomenon.

The results from the  $(\text{NH}_4)_2\text{SO}_4/\text{NH}_4\text{NO}_3$  mixture were more difficult to interpret. Most of the mixtures of different mole ratios that we have investigated showed absorption of water at low relative humidities. Thermodynamics and surface morphology alone are not sufficient to explain the data. The low crystallization point of  $\text{NH}_4\text{NO}_3$  may cause particles to exist as metastable aqueous droplets at low relative humidities even though the solid crystal is the thermodynamically favored state.

**Acknowledgment.** This research was supported by grants from the National Science Foundation (ATM-9422993) and the Environmental Protection Agency (R82-2980-010). Also, we would like to thank NATO for supporting the development of AIM2.

## References and Notes

- (1) Tang, I. N. In *Generation of Aerosols and Facilities for Exposure Experiments*; Willeke, K., Ed.; Ann Arbor Science Publishers: Ann Arbor, MI, 1980.
- (2) Tang, I. N. *J. Aerosol Sci.* **1976**, *7*, 361.
- (3) Tang, I. N.; Munkelwitz, H. R.; Davis, J. G. *J. Aerosol Sci.* **1978**, *9*, 505.
- (4) Tang, I. N.; Wong, W. T.; Munkelwitz, H. R. *Atmos. Environ.* **1981**, *15*, 2463.
- (5) Cohen, M. D.; Flagan, R. C.; Seinfeld, J. H. *J. Phys. Chem.* **1987**, *91*, 4575.
- (6) Cohen, M. D.; Flagan, R. C.; Seinfeld, J. H. *J. Phys. Chem.* **1987**, *91*, 4583.
- (7) Wexler, A. S.; Seinfeld, J. H. *Atmos. Environ.* **1991**, *25A*, 2731.
- (8) Chan, C. K.; Flagan, R. C.; Seinfeld, J. H. *Atmos. Environ.* **1992**, *26A*, 1661.
- (9) Koloutsou-Vakakis, S.; Rood, M. J. *Tellus* **1994**, *46B*, 1.
- (10) Potukuchi, S.; Wexler, A. S. *Atmos. Environ.* **1995**, *29*, 1663.
- (11) Potukuchi, S.; Wexler, A. S. *Atmos. Environ.* **1995**, *29*, 3357.
- (12) Ge, Z.; Wexler, A. S.; Johnston, M. V. *J. Colloid Interface Sci.* **1996**, *183*, 68.
- (13) Clegg, S. L.; Pitzer, K. S. *J. Phys. Chem.* **1992**, *96*, 9470.
- (14) Johnston, M. V.; Wexler, A. S. *Anal. Chem.* **1995**, *67*, 721A.
- (15) Carson, P. G.; Neubauer, K. R.; Johnston, M. V.; Wexler, A. S. *J. Aerosol Sci.* **1995**, *26*, 535.
- (16) Carson, P. G.; Neubauer, K. R.; Johnston, M. V.; Wexler, A. S. *Aerosol Sci. Technol.* **1997**, *26*, 291.
- (17) Neubauer, K. R.; Johnston, M. V.; Wexler, A. S. *Int. J. Mass Spectrom. Ion Processes* **1997**, *163*, 29.
- (18) Neubauer, K. R.; Johnston, M. V.; Wexler, A. S. Humidity effects on mass spectra of single aerosol particles. *Atmos. Environ.*, submitted.
- (19) Zhang, J.-Y.; Nagra, D. S.; Li, L. *Anal. Chem.* **1993**, *65*, 2812.
- (20) Mansoori, B. A.; Johnston, M. V.; Wexler, A. S. *Anal. Chem.* **1994**, *66*, 3681.
- (21) Vogt, R.; Finlayson-Pitts, B. J. *J. Phys. Chem.* **1994**, *98*, 3747.
- (22) Barraclough, P. B.; Hall, P. G. *Surf. Sci.* **1974**, *46*, 393.
- (23) Dai, D. J.; Peters, S. J.; Ewing, G. E. *J. Phys. Chem.* **1995**, *99*, 10299.
- (24) Mallina, R. V.; Wexler, A. S.; Johnston, M. V. *J. Aerosol Sci.* **1997**, *28*, 223.
- (25) Leong, K. H. *J. Aerosol Sci.* **1981**, *12*, 417.
- (26) Leong, K. H. *J. Aerosol Sci.* **1987**, *18*, 525.
- (27) Pruppacher, H. R.; Klett, J. D. *Microphysics of Clouds and Precipitation*; Reidel: Dordrecht, 1980.
- (28) Pandis, S. N.; Wexler, A. S.; Seinfeld, J. H. *J. Phys. Chem.* **1995**, *99*, 9646.
- (29) Middlebrook, A. M.; Thomson, D. S.; Murphy, D. M. *Aerosol Sci. Technol.* **1997**, *27*, 293.
- (30) ten Brink, H. M.; Veefkind, J. P. *J. Aerosol Sci.* **1995**, *26*, S553.
- (31) Rood, M. J.; Shaw, M. A.; Larson, T. V.; Covert, D. S. *Nature* **1989**, *337*, 537.
- (32) Thomson, D. S.; Murphy, D. M. *Appl. Opt.* **1993**, *32*, 6818.
- (33) Thomson, D. S.; Middlebrook, A. M.; Murphy, D. M. *Aerosol Sci. Technol.* **1997**, *26*, 544.